The low radioactivity link of the CUORE experiment

2009 JINST 4 P09003

(http://iopscience.iop.org/1748-0221/4/09/P09003)

PUBLISHED BY IOP PUBLISHING FOR SISSA

RECEIVED: *August 12, 2009*
ACCEPTED: *August 22, 2009*
PUBLISHED: *September 7, 2009*

The low radioactivity link of the CUORE experiment

E. Andreotti,[a,b] **C. Arnaboldi,**[b] **M. Barucci,**[c] **C. Brofferio,**[b] **C. Cosmelli,**[d] **L. Calligaris,**[b] **S. Capelli,**[b] **M. Clemenza,**[b] **C. Maiano,**[b] **M. Pellicciari,**[a,b] **G. Pessina**[b,1] **and S. Pirro**[b]

[a] *Dipartimento di Fisica e Matematica dell'Università dell'Insubria, Via Valleggio 11, Como I-22100, Italy*

[b] *INFN, Sezione di Milano-Bicocca and Dipartimento di Fisica dell'Università di Milano-Bicocca, P.za della Scienza 3, Milano 20126, Italy*

[c] *Dipartimento di Fisica dell'Università di Firenze and INFN, Sezione di Firenze, Firenze 50125, Italy*

[d] *Dipartimento di Fisica dell'Università di Roma La Sapienza and INFN, Sezione di Roma, P.le Aldo Moro 2, Roma 00185, Italy*

E-mail: Gianluigi.Pessina@mib.infn.it

ABSTRACT: CUORE will be an array of 988 TeO_2 bolometers ($5 \times 5 \times 5\,cm^3$) held at about 10 mK. It will study the very rare double β decay process from ^{130}Te. The electrical connections of the array to the room temperature electronics will consist in about 2000 wires. We will describe the design and characterization of the 3 interconnection sectors going from the detectors to the mixing chamber, the coldest stage at which the array is thermally and mechanically anchored, and from the mixing chamber to room temperature. The lower part consists of a set of 2.3 m long, 50 μm thick, Cu-insulator tapes having PEN (Polyethylene 2.6 Naphthalate) substrate, on which a pattern of copper tracks are etched. The differential layout pattern chosen allows obtaining a signal cross talk between adjacent channels of about 0.024%, together with a capacitance of about 26 pF/m and a resistance larger than 200 GΩ/m. On the top of the mixing chamber, Cu-Kapton boards are used to join the tapes to the second upward-going 2 m long links, implemented with twisted NbTi wires, interwoven in a NOMEX® texture. NbTi-NOMEX link features about 100 pF/m and negligible level of cross-talk. The radioactivity content of Cu-PEN tapes, Cu-Kapton boards, NbTi-NOMEX ribbons and connectors has been investigated and found to be compliant with the experimental requirements. A mechanical study has been done to quote the vibration transmission properties of the highly packaged tapes.

KEYWORDS: Cryogenic detectors; Special cables; Detector design and construction technologies and materials; Cryogenics and thermal models

[1] Corresponding author.

doi:10.1088/1748-0221/4/09/P09003

Contents

1 Introduction

CUORE, a Cryogenic Underground Observatory for Rare Events [1] is an experiment that will consist of 988 low temperature detectors. Each detector will be composed of a 750 g TeO_2 crystal on which a thermistor and a heater will be glued. With a base temperature of the crystals of about 10 mK a measurable temperature increase (0.7%) is foreseen for an energy release of 1 MeV by an impinging particle. This bolometric system is particularly suitable for the study of the neutrinoless double β decay, $0\nu\beta\beta$, of ^{130}Te (Q-value: 2527 keV [2, 3]), a very rare process to which CUORE will be dedicated: the abundance of ^{130}Te in natural TeO_2 is 28% in mass, therefore no expensive enrichment of the candidate isotope is strictly required, and tellurite is a very robust crystal, able to sustain many thermal cycles without showing stresses or defects.

The study of the $0\nu\beta\beta$ decay needs very stringent requirements on radioactivity for the materials located in close proximity to the detectors. This derives from the very low rate expected for the signals of the process under investigation. For this reason CUORE will be located under the Gran Sasso mountain to shield it from cosmic rays. The refrigerator, used to maintain the base temperature of operation below 10 mK, will be constructed with selected materials, having very low levels of radioactive contamination, and all the materials used near the detector will be carefully selected and checked.

In this paper we will describe the work done for the realization of the electrical link from the detector array to the outside world. The link we concentrate on is facing directly the detectors in its first part. Therefore, the amount of tolerated radioactivity for the chosen material for its construction is less than a mBq/kg in ^{238}U and ^{232}Th, to guarantee less than 10^{-3} counts/(keV kg y) in the region of 2.5 MeV, where the process under study is expected. The link must satisfy additional stringent electrical requirements: close packaging and negligible cross-talk. And last, but not least, thermal and mechanical studies have also been accomplished, to exclude that the readout system can couple mechanically the refrigerator vibrations to the detectors.

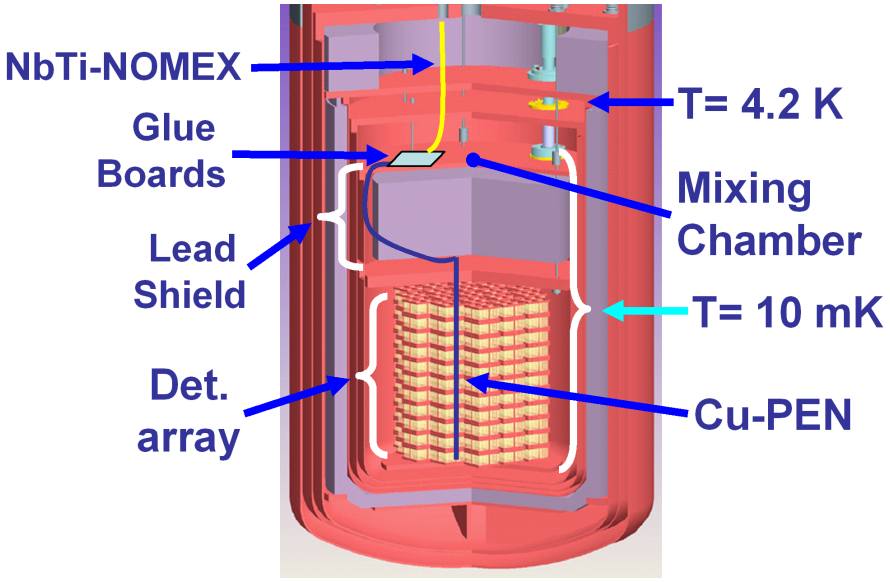

Figure 1. Artistic view of the cross-section of the experimental setup in the refrigerator of CUORE.

Cu-Kapton boards have also been designed and built, to connect the first (Cu-PEN) and second (Nb-Ti-NOMEX) stages of the link at the Mixing Chamber level. The boards and NbTi-NOMEX have a little bit less stringent background requirements, since they are located in a safer position, far away from the detectors.

All these requirements have been respected in the construction of the setup that will be described in details in the following.

1.1 System configuration and requirements

The CUORE detector array will be housed in a refrigerator designed on purpose, to reduce as much as possible radioactivity, together with having the necessary power to cool at very low temperatures (5–10 mK) a 1.6 ton detector and 10 tons of Pb at less than 1 K [4]. In figure 1 a schematic sketch of the detector inside the cryostat is shown. The detector array, composed of 76 columns, grouped by fours in tower-like structures, with 13 bolometers per column, is located at the bottom of the refrigerator and thermally anchored to the Mixing Chamber (MC) the coldest part of the system. Between the array and the bottom plate of the MC there is a 30 cm thick disk of lead for γ-ray shielding purposes. Another 6 cm of lead surrounds the lateral and bottom sides of the array. Lead is a good shield against γ-rays thanks to its high Z and density. The base material of the refrigerator and of the array supports is oxygen-free copper, with a very low level of radioactive contaminants [5]. A compact interconnection system is foreseen to assure the readout of every detector up to the top of the refrigerator, where the first stage of the electronics is located. The link consists of 988 pairs of wires, 1976 in total, to perform a differential readout for every detector. Each crystal has also a small heater (a heavily doped Si resistor [6]) glued on it, to which a small voltage pulse is applied every few minutes to release a tiny Joule power into the crystal that simulates the effect of an impinging particle. These events are used to stabilize the system gain continuously. Heaters from one column are all connected in parallel. Consequently only 152 wires are needed for this latter feature.

In figure 1 the readout routing for two columns is shown: 3 Cu-PEN tapes are used to connect the 26 thermistors. Another tape is used to connect the heaters of the same 26 crystals. The tapes are packed together, putting one on top of the other. Between any pair of them a grounded tape is inserted for electrical shielding, therefore totaling 9 tapes. Along the towers and below the Cu disk from which all the towers are suspended, the tapes are almost completely covered by oxygen-free copper, to protect against the possible presence of α-emitting contaminants on the tapes themselves. These would otherwise impinge on the crystals directly. From the Cu disk to the top of the mixing chamber the tapes curve around the lead shield, without any cover. In this region the α radioactivity is no longer a problem for the detectors.

This set-up has to meet several stringent requirements: each tape must have a small width and thickness because the available space is limited, the materials applied should be carefully selected in respect to contaminations of α- or γ-particle emitters, total mass should be minimized to keep the lowest possible level of background radioactivity.

Above the MC a set of glue boards are present that connects the Cu-PEN with the NbTi-NOMEX ribbon system with which the upper link is implemented. The NbTi-NOMEX system must undergo a thermal gradient of 300 K and was therefore selected for its small thermal conductance characteristic.

2 Low background material selection

In ^{130}Te $0\nu\beta\beta$ searches (Q-value: 2527 keV), the most important contaminants that may impair the experiment are those that can decay emitting α- or γ-particles above 2.5 MeV. Since α mean free path is very small in matter, they contribute to detector background only if originated on the materials that face it or on the surface of the detector itself, that deserve a very accurate cleaning. Shielding of γ-rays on the contrary is much more difficult and requires high density, large Z materials, with enough thickness. The most dangerous contaminants that could be present in all used materials are the natural radioactivity chains (coming from ^{238}U, ^{235}U and ^{232}Th), with their long-living daughters, together with ^{60}Co and ^{40}K (this last one in fact emits lower energy γ's, so is less important). Only very small concentrations of these elements are admitted for all the materials present near the array, going from pg/g to ng/g for U and Th, down to only 10^{-22} g/g in ^{60}Co. Higher levels of contaminations would spoil the CUORE experiment sensitivity, which aims at studying the inverse hierarchy region of the neutrino mass scale through the study of $0\nu\beta\beta$ [7].

To measure the radioactivity of our materials, several systems are employed. For α-spectroscopy, 30% intrinsic efficiency coaxial HPGe detectors located under the Baradello hill in Como [8] and in our laboratory in Milano were used for preliminary discrimination. When higher sensitivity is required, 100% intrinsic efficiency coaxial HPGe detectors, located under the Gran Sasso Mountain, are preferred. For α-spectroscopy several Si (surface barrier) detectors are used, mainly in Milano.

The first material taken into consideration for the readout near the detector was twisted Cu wires interwoven with a NOMEX texture, that has already been applied in low temperature systems (SCUBA and SCUBA-2 detectors [9]). Unfortunately, the NOMEX matrix has shown to be too radioactive for our purposes (see table 1), even if it was considered good enough for the higher part of the cabling. Finally, NbTi-NOMEX ribbons will be used from the MC to the room tem-

Table 1. Background level for γ contamination of the materials considered in the design of the link. NM=Not Measured, BL=Limited from environment background.

	^{238}U mBq/kg	^{232}Th mBq/kg	^{40}K mBq/kg	^{137}Cs mBq/kg
NOMEX	21	19	2130	< 3.3
Cu-Mylar	BL	BL	BL	2060 ± 460
Cu-PEN	< 1.3	< 1.0	< 13.2	< 0.36
PTFE-15%	8300 ± 500	14100 ± 200	7300 ± 300	
Cu-Kapton	< 30	31 ± 15	< 118	< 8.2
Fiberglass	26800 ± 1550	23750 ± 2610	10700 ± 630	NM
	^{238}U mBq/pin	^{232}Th mBq/pin	^{40}K mBq/pin	
Micro-D	0.1	0.15	0.01	NM
ZIF	0.2	0.3	0.3	NM
SSC	0.3	0.4	0.6	NM

perature region. We then considered Cu-insulator tapes on which very dense thin Cu strips can be laid-out, reducing as much as possible the number of tapes required. Two substrates were taken into consideration: PEN (Polyethylene 2.6 Naphthalate) and Mylar, both with well-known bulk purity. Cu-PEN showed a very low α- and γ-activity, while the sample of Cu-Mylar showed an important contamination in ^{137}Cs, after a first rough measurement in the Milano Laboratory, and was therefore discarded.

For the MC glue Printed Circuit Boards (PCBs), we discarded the choice of classical fiberglass, which is usually contaminated in Th and U. Instead, two other materials PTFE-15% reinforced fiberglass and Kapton were considered. As expected, the first one showed a higher activity, while Kapton has some contamination if compared with PEN (for which we extracted only limits), that was found acceptable since PCBs will be located above the lead shield.

In parallel to the substrate study our program included also the characterization of some selected connector types to be used on the glue board: Micro-D, ZIF and Standard Straight Connector (SSC). The selection was made on past experience from EDELWEISS [10] and CRESST [11] collaborations. Data from our γ-background tests are reported in table 1 as mBq/pin, which is in this case more relevant, while α contamination study was not necessary since connectors will be placed above the MC.

After that PEN was selected, ZIF connectors were the only available choice for the lower stage link, since soldering Cu on PEN is not possible. ZIF has the advantage to require only the female connector that directly crimps the PCB and therefore can afford a higher radioactivity level by a factor of 2. Taking this into account, we decided to use ZIFs also for the upper stage link, terminating the NbTi-NOMEX wires on a special Cu-Kapton PCB (see figure 11)).

In table 1 γ contamination levels or limits are quoted for the described materials. A Monte Carlo code has been run in each measurement configuration, to extract the efficiency needed for the evaluation of the activity of the specimen.

Table 2. Background level for α contamination of the materials considered in the design of the link. NM=Not Measured.

	^{232}Th $[10^{-6}\,\mathrm{Bq/cm^2}]$	^{238}U $[10^{-6}\,\mathrm{Bq/cm^2}]$	^{210}Pb $[10^{-6}\,\mathrm{Bq/cm^2}]$
Cu-Mylar copper side	< 0.39	< 0.56	(7.5 ± 0.8)
Cu-Mylar mylar side	$(0.70 \pm .22)$	< 0.49	< 1.1
Cu-PEN copper side	< 0.51	< 0.60	< 6.5
Cu-PEN PEN side	< 0.52	< 0.54	NM

The evaluation of the background from α-particles, shown in table 2, is important only for PEN and Mylar since they were the candidates to face directly the detectors and the tapes will be not completely covered from Cu.

3 Link set-up and characterization

The results on the background measurements shown in the previous section suggest the adoption of PEN and Kapton as substrates for our readout links at base temperature. An accurate design and specific technological solutions were adopted for both, due to the non standard requirements. The set-up was produced in close collaboration with industry.[1] The upper section of the link was implemented with NbTi-NOMEX.

3.1 Cu-PEN based flat flexible tape

The Cu-PEN which forms the lower stage of connection of the array must satisfy different specifications: low background, negligible cross-talk, negligible microphonism, very large real and complex parts of the parasitic impedance and high level of packaging.

The detectors of CUORE are being read by differential voltage amplifiers. The link layout is designed to reduce as much as possible the distance between the two tracks of every differential pair, so any mechanical vibration generates equal effects (common mode) on both elements of the pair. Therefore, at the amplifier input, the disturbances will cancel out. Cross-talk is minimized by the differential readout if the remote inducing signals generate the same effect on the capturing nodes of a pair. This is possible if the distances between the source of the cross-talk and the two capturing nodes are similar. The Cu-PEN was designed to account for all these specifications.

Figure 2 is the mosaic composition of the Cu-PEN implemented. At its top there is the row of 30 pads which form the male-connector that will fit the female-ZIF connector on the Kapton board at the mixing chamber level. At its bottom we have the left-right legs with the bonding pads for the connection of thermistors/heaters (there will be more than one of these in each cable). Two pairs of

[1] Tecnomec srl, http://www.pcb-tecnomec.com/.

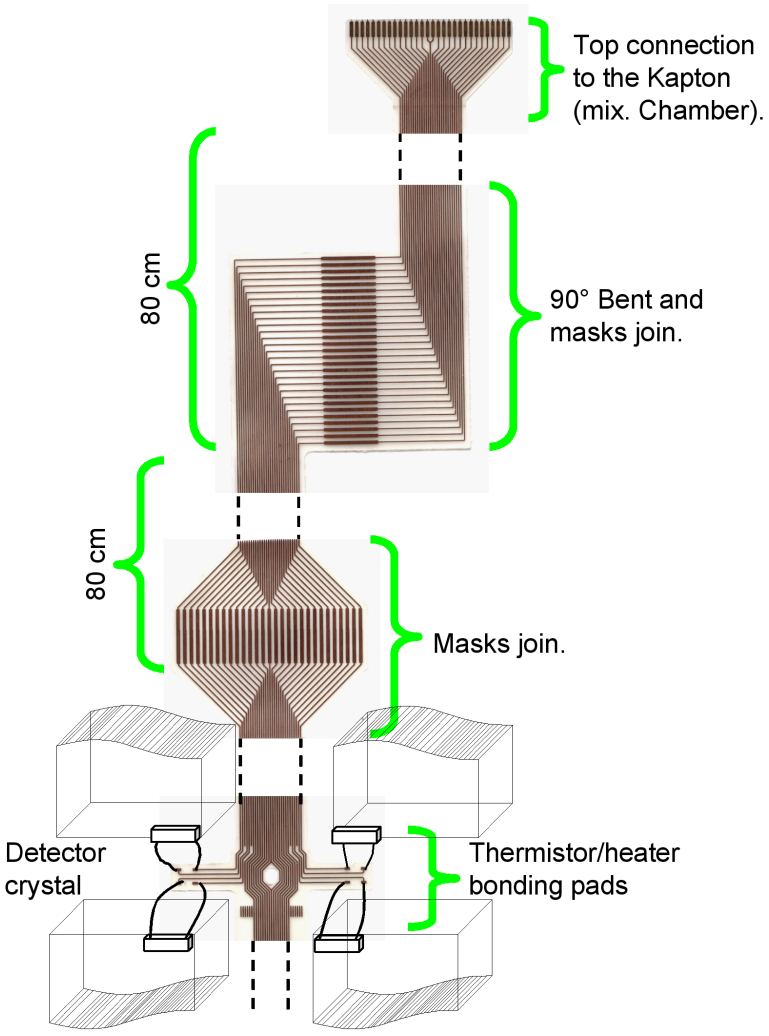

Figure 2. Mosaic composition, not to scale, of the ribbon cable with the critical parts evidenced. At the bottom an example of detector connections is shown.

pads on top of the left-right legs will connect the thermistors/heaters of two crystals on the upper floor with the ball-bonding soldering. Two pairs of pads at the bottom will connect those in the lower floor.

Twenty-nine tracks are routed parallel to each other along the tape. Pads # 15–16 of the male-connector are routed to the same central track (GND). The width of every track is 0.2 mm and the pitch 0.4 mm. The final width of the ribbon is 13.4 mm, with 1 mm on each side of unrouted margin.

Our final flexible cable will be 2.3 m long, while the standard production masks for track serigraphy have an extension of 80 cm maximum. Therefore 3 masks must be jointed by hand. To avoid any possible failure, at the joints the Cu-PEN was shaped wider on purpose and the tracks are larger (0.4 mm) and well separated (0.8 mm the pitch). Examples of this feature are the "Mask joint" and the "90^{o} Bend and Mask joint" of figure 2. In the latter situation we add a mask joint in correspondence of a mechanical bend. The flexible tape supports 10 differential channels (20 tracks) with a ground track between adjacent channels (9 tracks) to improve cross-talk rejection. It was accurately characterized both for its impedance and dynamic performances.

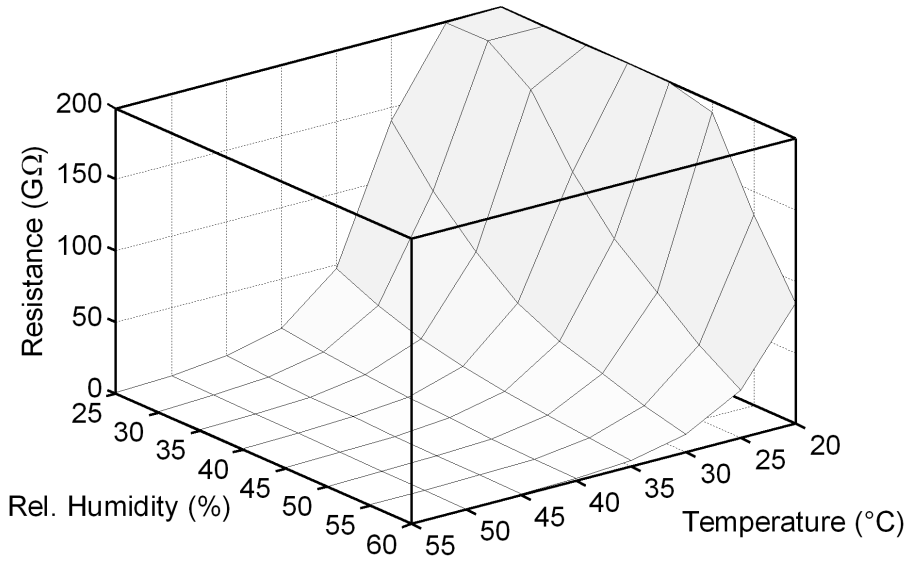

Figure 3. Static parasitic impedance between a pair of adjacent tracks. The full scale achievable was 0.2 TΩ. Minimum measured values were a few hundreds MΩ at the higher temperatures and RHUs.

The impedance characterization consisted in the measurement of the capacitance and resistance between the tracks. Knowledge of the inductance was not necessary since the small bandwidth of the detector signal, 10 Hz, limited by the thermal time constants.

The static impedance is a very important parameter since it can add DC offset and parallel noise. It was measured following two different procedures. A preliminary study was made on the influence of temperature and Relative Humidity, RHU, on its value. Then, a characterization was made in vacuum, its final operating environment.

The Cu-PEN tapes were put in an environmental chamber, Vötsch VC 4018. The temperature and the RHU were varied and the impedance of 2 adjacent tracks on each specimen was measured with the Keithley 6514 Electrometer, after equilibrium conditions were reached at each step. Figure 3 is a 3D-plot of the results. The impedance was found to be very large when the RHU was smaller than about 40% and the temperature equal to or lower than 20 °C. In these operating conditions the parasitic impedance was larger than the instrumental full-scale limit of 200 GΩ: an excellent figure.

If temperature and/or RHU grow, the impedance undergoes a dropout. This is an important indication of the poor level of accuracy that can be achieved with a direct measure during the installation in the refrigerator, in typical lab conditions.

The Cu-PEN parasitic impedance was also measured versus vacuum level at room temperature. Even 0.1 bar of depression with respect to ambient was enough to exceed the instrument full-scale limit. This result suggests to use the procedure of preliminary pumping before testing the readout.

Capacitance between tracks has been measured with the Agilent 4284A LCR-meter. We model

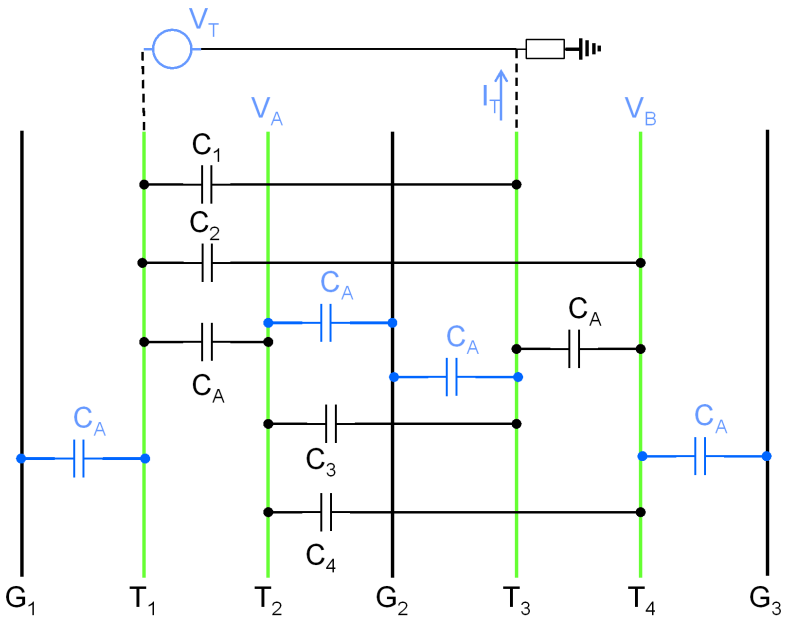

Figure 4. A pair of differential tracks: T_1–T_2 and T_3–T_4 and their shields, G_1 to G_3 of the flexible cable of figure 2. All the capacitances needed to model the system are indicated. In the upper part the set-up for the characterization of the impedance between tracks T_1 and T_3 is shown.

the system of two pairs of differential tracks as in figure 4. An example of the characterization of the capacitance between tracks T_1 and T_3 is shown. The LCR-meter measures using the 4-wires method. The impedance quoted is therefore the ratio V_T/I_T, where the return current I_T is that flowing only in T_3, in the example shown. We took data in two configurations. In the first case tracks G_x's have been left floating, while in the second case they have been grounded. Capacitances between tracks T_1 and T_2, C_{12}, between tracks T_1 and T_3, C_{13}, etc. have been measured. When G_x's were left floating, the impedance between T_1 and G_2 was measured too.

The Diamond-markers of figure 5 are the results obtained in the case with G_x's floating. Capacitances are quoted per unit length. We fitted the data with a power law of the inverse of the track pitch, obtaining an exponent close to 0.8. The same procedure has been applied when the G_x's were grounded. Data are represented with star-markers in figure 5. Looking at their fit we now find an exponent for the power law almost equal to 2. The improvement can be attributed to the shielding effect consequential to the grounding of the G_x's.

From figure 5 it can be seen that the capacitance of a pair, for instance C_{12}, is 16.6 pF/m after G_x's grounding, an adequate figure with respect to the detector characteristics. The figure obtained with G_x's floating is 26 pF/m. The effect is easily interpreted from the model of figure 4. Capacitance C_{12} is not equal to C_A, because we must consider also its paralleling to the series combination of C_1 and C_3, C_2 and C_4, the capacitances C_A of the other tracks and the sets of symmetrical tracks on the left of T_1 and T_2, not shown in the figure. Since C_1, C_2, etc. are greatly affected by shielding, the same outcome is observed on C_{12}. Solving the mesh equations for C_{12} a rational-polynomial in C_A is obtained, the numerator resulting in a 4^{th} grade polynomial, while the denominator in a 3^{rd} grade.

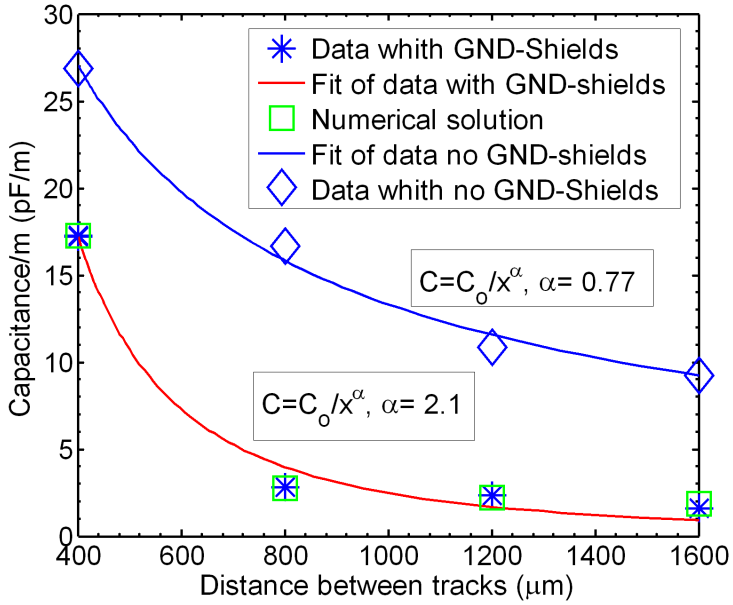

Figure 5. Capacitance vs. the distance between the centers of the tracks (pitch). Diamonds are the measurements taken with the shields left floating, while stars are the same measure with the shields grounded. Squares are the numerical fits for the latter configuration.

The same considerations obtained for C_{12} apply to C_{13}, C_{23}, etc. Solving the mesh equations also for all these cases we obtain a second order rational-polynomial in C_A in both the numerator and denominator. An easy estimation can be obtained from figure 4, with all G_x's grounded, if we assume $C_A \gg C_i$, $i = 1, \ldots$:

$$\begin{cases} C_{12} = C_A \\ C_{13} = C_1 + \frac{C_2}{2} + \frac{C_3}{2} + \frac{C_4}{4} \\ C_{14} = C_2 + \frac{C_1}{2} + \frac{C_3}{4} + \frac{C_4}{2} \\ C_{23} = C_3 + \frac{C_1}{2} + \frac{C_2}{4} + \frac{C_4}{2} \\ C_{24} = C_4 + \frac{C_1}{4} + \frac{C_2}{2} + \frac{C_3}{2} \end{cases} . \tag{3.1}$$

In (3.1) the terms 1/2 and 1/4 arise from the signal partitions at the nodes by C_A's. The approximation used in (3.1) is not adequate for cross-talk evaluation since the latter is a second order effect. To approach the problem given by the difficulty in solving the algebraic system of 5 equations, we adopted a numerical solution in which we assumed that capacitances C_i, $i = 1, \ldots, 4$, have the same power law dependence on the inverse of the pitch, since they all include one grounded track in between. The same was not considered for C_A. In this way we reduced to 3 the number of unknown variables. In addition we considered in the system also the equation governing the measurement of cross-talk, as depicted in figure 6, of easy mathematical solution, as we will see below. A system consisting of 6 equations with 3 unknown variables was at the end numerically solved. Results are summarized in table 3, where the measured capacitances are quoted for comparison. Using the calculated values of table 3 in the system of equations governing figure 4 the squares-markers of figure 5 are obtained that match the measured data very well.

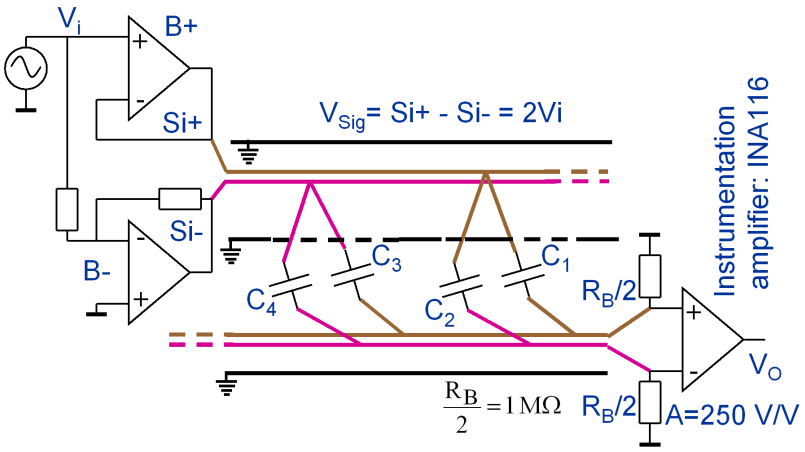

Figure 6. Measurement set-up for the characterization of the cross-talk of adjacent pairs within the cable. The relative position of the tracks in the sketch is only to guide the eyes and does not respect the actual layout.

Table 3. Measured and calculated capacitances from figure 4, G_x grounded. C_1 to C_4 has been modelled with C1(d13/dij)$^{\alpha}$, where α resulted to be 1.57. Capacitance values are expressed in pF/m.

	C_{12}	C_{13}	C_{14}	C_{23}	C_{24}	C_{cr-tk}
Measured	17.25	2.35	1.56	2.79	2.31	−0.49
	C_A	C_1	C_2	C_3	C_4	C_{cr-tk}
Calculated	16.65	0.93	0.59	1.75	0.93	−0.48

Dynamic performances may be affected in two ways. The parasitic capacitance between the two tracks of a differential channel may create excessive signal integration, while the parasitic capacitance between different channels may create excessive level of cross-talk signal. Assuming a detector dynamic impedance of about 50 MΩ and a parasitic capacitance per meter 1.5 times that quoted in the first column of table 3 (since the parasitic capacitance is C_A approximately shunted by $C_A/2$) we get a limit of about 55 Hz for the frequency bandwidth for a 2.3 m Cu-PEN tape. This frequency is much larger than the bandwidth of a standard detector of CUORE, which rarely exceeds 10 Hz.

The last column of table 3 is C_{cr-tk}, the capacitance responsible for the cross-talk signals. It was measured with the set-up of figure 6, that simulates the worst case. A differential signal is applied to a paired track, starting from the input V_i, using a unity gain buffer amplifier, B+, and a unity gain inverting buffer amplifier, B-. The capturing pair is readout with an INA116, an instrumentation differential amplifier for which the voltage gain was set to 250 V/V. A pair of 1 MΩ resistors, accurately matched, simulates a detector thermistor having dynamic impedance, R_B, of 2 MΩ. The Common mode rejection ratio of the reading structure was negligible compared to that expected from the Cu-PEN. The input V_i was generated with an arbitrary function generator. Its shape was chosen similar to the typical signals of some representative detectors of CUORICINO [12], the pilot experiment of CUORE.

The time constants of the experimental set-up of figure 6 are much smaller than those of the simulated detector signals. At first approximation we can neglect the voltage drop across resistors

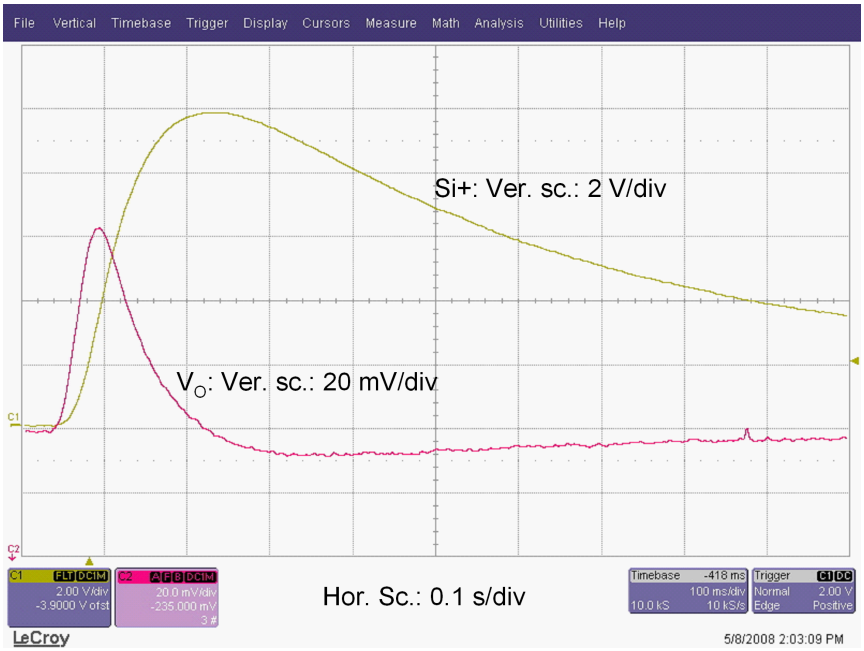

Figure 7. Screen shot from the oscilloscope of the signal at the B+ output and the V_0 output of the differential amplifier INA116 of figure 6.

R_B compared to those across capacitors C_i. The influence of capacitors C_A is also negligible, under this approximation. At the output of the amplifier V_0 will be, in the frequency domain ($s = j\omega$):

$$\begin{aligned} V_0(s) &\approx sA\left[(C_1 - C_2) - (C_3 - C_4)\right]\frac{R_B}{2}\frac{V_{\mathrm{Sig}}(s)}{2} \\ &\approx sA\frac{R_B}{2}C_{\mathrm{cr-tk}}\frac{V_{\mathrm{Sig}}(s)}{2} \end{aligned} \tag{3.2}$$

Remembering that s is the derivative operator, in the time domain we have:

$$V_0(t) \approx A\frac{R_B C_{\mathrm{cr-tk}}}{4}\frac{dV_{\mathrm{Sig}}(t)}{dt} \tag{3.3}$$

From (3.3) we see that the differential readout makes the cross-talk a partially common mode disturbance, as indicated by the presence of the factor 1/4.

The experimental proof of (3.3) is the oscilloscope screen shot of figure 7, where both the input and output signals of figure 6, taken from a 3 m long specimen, are shown. The cross-talk signal is very close to the derivative of the inducing signal, as one can appreciate looking at figure 8, where the measured cross-talk signal, down-loaded from the scope, is plotted, together with the numerical derivative of the input signal, with amplitude and offset fitted to the measured one. Both signals are referred now to the INA116 inputs.

The measured signal is very close to the shape of the calculated one. This means that any parasitic static impedance has negligible effects and can be considered of very large value. From (3.3) and the parameters obtained from figure 8 the cross-talk capacitance $C_{\mathrm{cr-tk}}$ results to be less than 0.5 pF/m. Its actual value is reported in table 3 and can be compared with the corresponding value computed from the model of figure 4 and the measurements taken with the LCR meter. Again a

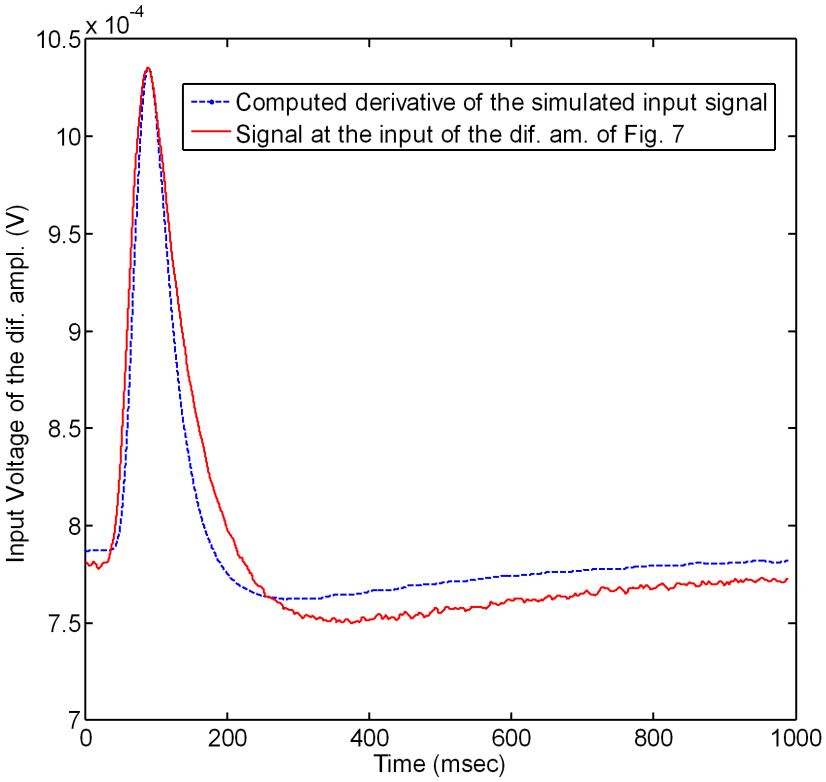

Figure 8. Cross-talk signal resulting from the set-up of figure 6 referred at the input of the INA116 amplifier, full-line. Derivative of the input signal of figure 6 fitted in amplitude and offset to the measured signal, dotted-line.

good match has been verified. To quote the good rejection properties of the flat cable we estimate, for a released energy of 10 MeV in one detector, about 2400 eV — equivalent of fake signal on the near detector, or 0.024%.

The derivative of the detector signal is proportional to the inverse of its rise time, t_r, constant, τ_r ($t_r = 2.2\tau_r$), multiplied by the parameter α. The last one accounts for the amplitude at the maximum. At first we can approximate the derivative signal in figure 8 with the difference of 2 exponentials having time constant ratio between 5 and 10, from which α results between 0.5 and 0.6. The cross-talk amplitude V_{cr-tk} can therefore be given from (3.3) as:

$$V_{cr-tk}(t_{max}) \approx \frac{R_B C_{cr-tk}}{4} \frac{1}{\tau_r} \alpha \tag{3.4}$$

The upper value is obtained when τ_r is limited by the parasitic capacitance, $\tau_r \approx R_B C_{PAR}$, from which we get $\alpha C_{cr-tk}/4C_{par} \approx 0.24\%$, when C_{cr-tk} is roughly 0.5 pF/m from table 3 and C_{PAR} equals $3/2C_A$, or 26 pF/m. This last quoted parameter is the very worst case, achievable only when fast detectors are considered, which is not the situation for CUORE.

The CUORE array will need in total $\sim$ 150 Cu-PEN flexible flat tapes and $\sim$ 180 PEN-based ground shields to route all the thermistors and heaters. The presence of the shield tapes in the final packaging will increase the capacitance of every pair and will improve further the cross-talk between close channels.

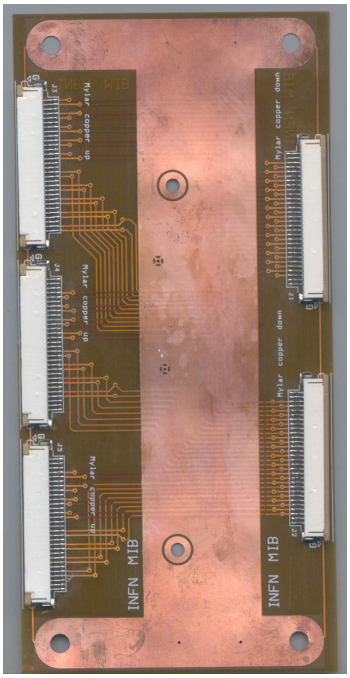

Figure 9. Kapton glue board. On both left and right sides the 30-pole female ZIF input/output connectors are visible.

3.2 Kapton based glue boards

The wiring requirements for the colder (lower) and warmer (upper) parts of the refrigerator are different. In the colder part, below the MC and close to the detectors, there is no temperature gradient. Consequently the metal that composes the conductive tracks can be copper because its good thermal conductance will not heat-load the detectors.

From the mixing chamber to the outside of the refrigerator a thermal gradient of about 300 K is present. It is therefore very important that the thermal conductance of the link in that section be as small as possible. To this aim a system of NbTi wires interwoven with a NOMEX®[2] texture will be adopted.

Figure 9 shows the glue board that connects the Cu-PEN flat tapes coming from the detectors to the NbTi-NOMEX cables. The Kapton-board transmits the electrical signals between the two systems, and represent the last thermalization stage for the wires coming from the upper (warmer) part of the cryostat. To do this a large area of copper has been created on the top and the bottom of the board, shown in figure 9. In two inner layers the electrical connections are routed. The board is sandwiched along the copper regions between two copper heat sinks in good thermal contact with the MC. In this way a thermal short-path is made that avoids the transmission of heat to the detectors.

To be consistent with the layout of the Cu-PEN tapes, the connections are realized in pairs, with a ground track between every pair. The thickness of each of the 4 layers of the Kapton board of figure 9 is about 40 μm. If the ground tracks and copper areas are left floating, the capacitance

[2]Tekdata is the NbTi-NOMEX manufacturing company.

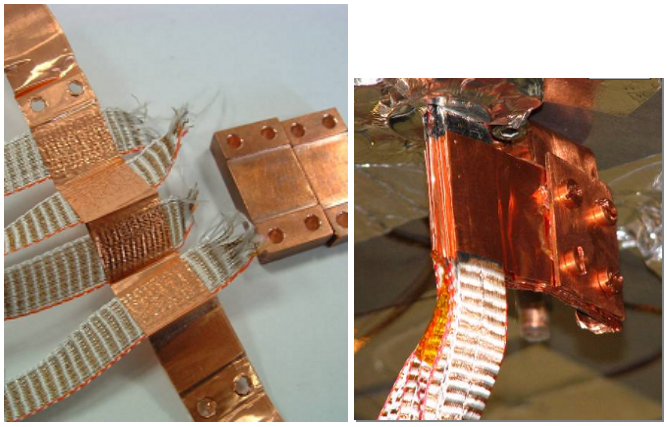

Figure 10. Thermalization stages at the 4.2 K for the NbTi-NOMEX cables. Some cables are individually embedded in Cu sheets on the left picture. The Cu sheets are superimposed each other and pressed in the final layout of the picture on the right.

between a pair of tracks is about 20 pF, which becomes less than 1 pF when the ground tracks are grounded. But in this situation the capacitance between any of the 2 tracks and ground is, as expected, the double of the previous case, 40 pF. Dynamically speaking the detector shunting capacitance is about 20 pF. These measurements have been done with an exerted pressure of about 2 Kg, simulating the final sandwiching effects. The measured capacitance is between 5% to 10% of the parasitic capacitance of the overall link, estimated to be around 400 pF. Increasing a factor 2 the thickness of the layers of the Kapton allows reducing by a corresponding factor the capacitance. Nevertheless we prefer to maintain this layout solution that allows for a much better and safer thermalization.

Every Kapton board manages 3 Cu-PEN tapes from one side, and two NbTi ribbon cables from the other. 3 sandwiched Kapton boards are required for each tower and groups of 9–12 boards are piled up on the mixing chamber. Five of such groups are foreseen for a total of 57 boards.

3.3 NbTi-NOMEX connecting link

From the MC to the outside of the refrigerator a thermal gradient of 300 K is present. As described in the previous sections, a system of woven ribbon cables with 13 twisted pairs of NbTi wires (100 μm of diameter) with a NOMEX® texture will be adopted. NbTi is a poor thermal conducting metal above 10 K and a superconducting material below, featuring very little heat transport in both conditions.

The expected scheme for the upper part of the link, from 300 K down to 4.2 K, foresees 5 identical straight tubes for the thermistor signals, with 16 NbTi-NOMEX ribbon cables each, and one straight tube for the heater signals and spare temperature sensors with 20 NbTi-NOMEX ribbon cables, all to be inserted from special Room Temperature ports

On the 4.2 K cold plate of the cryostat there is the first set of thermalization stages (see figure 10) for this part of the link, composed of sandwiches of copper plates and annealed Cu thin layers that perform good thermal contact between the wires and the copper plates. From the 4.2 K plate down to the MC the ribbon cables are thermalized also at 700 mK and 50 mK with similar

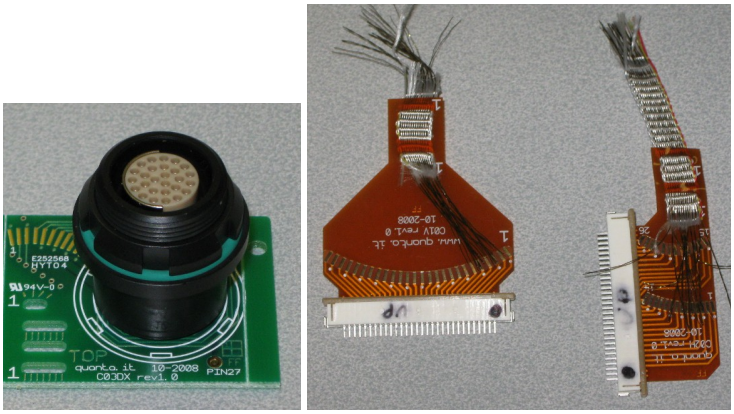

Figure 11. Vacuum connector from inside to outside the fridge mounted on its PCB (left). Termination example of the NOMEX® ribbon cable partially assembled on Kapton PCBs and inserted into ZIF connectors (right).

setups. From the 50 mK region the ribbons follow the last path towards the glue kapton boards, at the MC level, where, as seen in the previous section, they are subjected to the last thermalization stage. The dissipated power for the total wiring system on the 4 thermalization stages is expected to be around 0.2 W, 30 μW, 1 μW and 5 nW. The last one is an excellent figure, since the requirement was to not dissipate more than 1 μW at level of the mixing chamber.

Our NbTi wires have a Monel cladding and a Polyimide insulation, which allows a configuration of twisted pairs with about 500 twisting/m. The link was characterized both electrically and dynamically. Parasitic resistance between the wires of a pair resulted limited by the full scale of the Electrometer. Capacitance of a twisted pair was measured to be 100 pF/m, while the capacitance between two closed pairs was 25 pF/m. Cross-talk was characterized with the same set-up of figure 6. It was at the limit of the amplifier, found in excess of 97 dB. This excellent figure is due to the very close packaging of the twisted wires. This figure allowed avoiding the adoption of the guard wire for the NbTi-NOMEX.

The layout of the ribbon can be seen in figure 11. On the top of the fridge the NbTi wires are soldered on a PCB (fiberglass made) mounted on the vacuum connector, figure 11-left. At the mixing chamber the NbTi wires are soldered on a small Kapton board, figure 11-right side, terminated with a male row connector that fits the small ZIF on the glue board of figure 9.

4 Mechanical characteristics of Cu-PEN tapes

The flexible cables are assembled in packets of 18 Cu-PEN tapes for each tower, connected mechanically from the MC to the detector frames.

We have to assure that the rigidity of the Cu-PEN packaging and their elasticity do not transmit mechanical vibrations to the detectors coming from the upper system. A series of vibration tests has been performed on a prototype representing the connection between the MC and the tower top plate. We have tested a packet composed by seven 85 μm Cu-PEN tapes+seven Copper-mesh tapes, and a packet composed by 20 full copper 50 μm tapes. The length was 300 cm for each packet and the width ranging from 13 to 10 mm. The packet was shaped as it will be in the fi-

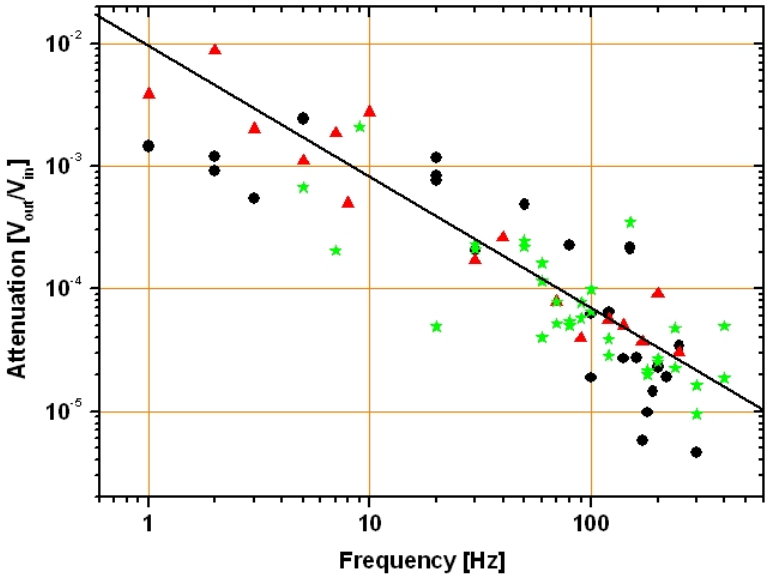

Figure 12. Measured mechanical attenuation of different Cu-PEN tape packet configurations vs. the excitation frequency, connected to a 5 kg free mass. The spread/colors represent subsequent measurements using different clamping techniques, see text.

nal experimental layout. The mechanical transfer function has been evaluated by the ratio of the acceleration measured by two accelerometers mounted on the upper end of the tape, where a mechanical excitation was applied, and on a freely suspended 5 kg plate, where the other end of the tapes was connected. The two accelerometers were Bruel & Kijaers calibrated accelerometers; the accelerometers have been inter-calibrated in the frequency range 0.5–300 Hz showing the same output within 10% from 0.5 to 100 Hz, and within 20% from 100 to 300 Hz. In figure 12 we show the measured mechanical attenuation for a typical Cu-PEN tape packet versus the excitation frequency. The spread/colours represent subsequent measurements where different clamping techniques have been used: the 14 PEN layers have been clamped in horizontal position and then bent at 90^o, or bent and then clamped, to keep the layers as close as possible. Moreover each measure has been repeated to test the reproducibility of the connection between the packets and the mass.

Although the data have some spread, the overall fit is close to 1/f, limited by the sensitivity of the accelerometer below 1 Hz. The Cu-PEN package behaves as a low pass mechanical filter with about 20 dB/dec roll-off and an attenuation smaller than -60 dB at 10 Hz, the signal bandwidth of the detectors of CUORE. That obtained is a good figure, more than adequate for CUORE. This result allows a quite flexible mounting procedure and a not too tight requirement on tape lengths and assembling.

5 Conclusions

The wire routing of the cold section of the readout for the 988 detectors of the CUORE cryogenic experiment has been designed, prototyped and is now under production. It consists of three sections. The first is the coldest one composed of $\sim 350 \times 2.3$ m long Cu-PEN (Polyethylene 2.6

Naphthalate) based flexible flat cables designed to minimize radioactive background, microphonics noise and cross-talk between channels. 57 4-layers glue boards, Kapton-based, are located on the Mixing Chamber, piled-up in 5 groups. Each one links two or three Cu-PEN to the third stage link, going from base temperature to room temperature, obtained by 13 twisted NbTi pairs of wires, interwoven in a NOMEX® texture.

An adequate level of radioactivity and a negligible level of cross-talk ($< 0.024\%$) has been figured by the link, despite the very high level of packaging.

Acknowledgments

We are indebted to Ing. Sandro Pigato and Ms. Eugenia Fornaro of Tecnomec: their invaluable support was essential for the realization of the presented set-up. We thank Mr. A. De Lucia for his accurate layout of the PEN and Kapton based circuit designs.

This work was partially supported by the Italian Ministry for University and Research, under contract 2006028149_003

References

[1] C. Arnaboldi et al., *CUORE: a cryogenic underground observatory for rare events*, Nucl. Instrum. Meth. **A 518** (2004) 775;
Cryogenic Underground Observatory for Rare Events, http://crio.mib.infn.it.

[2] M. Redshaw et al., *Masses of ^{130}Te, ^{130}Xe and double-β-decay Q value of ^{130}Te*, Phys. Rev. Lett. **102** (2009) 212502.

[3] N.D. Scielzo et al., *Double-β decay Q values of ^{130}Te, ^{128}Te, and ^{120}Te*, Phys. Rev. **C 80** (2009) 025501 [arXiv:0902.2376].

[4] A. Nucciotti et al., *Design of the Cryogen-Free Cryogenic System for the CUORE Experiment*, J. Low Temp. Phys. **151** (2008) 662.

[5] M. Laubenstein et al., *Underground measurements of radioactivity*, Appl. Radiat. Isotopes **61** (2004) 167.

[6] A. Alessandrello et al., *Methods for response stabilization in bolometers for rare decays*, Nucl. Instrum. Meth. **A 412** (1998) 454.

[7] A. Strumia and F. Vissani, *Implications of neutrino data circa 2005*, Nucl. Phys. **B 726** (2005) 294.

[8] C. Brofferio et al., *Characterization of an underground site in Northern Italy in view of low radioactivity measurements*, J. Environ. Radioact. **71** (2004) 159.

[9] D.M. Alexander et al., *Weighing the Black Holes in $z \approx 2$ Submillimeter-Emitting Galaxies Hosting Active Galactic Nuclei*, Astron. J. **135** (2008) 1968;
SCUBA 2, http://www.roe.ac.uk/ukatc/projects/scubatwo/.

[10] EDELWEISS collaboration, S. Fiorucci et al., *Identification of backgrounds in the EDELWEISS-I dark matter search experiment*, Astropart. Phys. **28** (2007) 143 [astro-ph/0610821];
Edelweiss-II, http://edelweiss.in2p3.fr/.

[11] G. Angloher et al., *Limit on WIMP dark matter using scintillating $CaWO_4$ cryogenic detectors with active background suppression*, Astropart. Phys. **23** (2005) 325 [astro-ph/0408006];
CRESST, http://www.cresst.de/.

[12] C. Arnaboldi et al., *Results from a search for the $0\nu\beta\beta$-decay of ^{130}Te*, Phys. Rev. **C 78** (2008) 035502.